Jet Noise Shielding Provided by a Hybrid Wing Body Aircraft

Michael J. Doty[1], Thomas F. Brooks[2], Casey L. Burley[3], Christopher J. Bahr[4], and Dennis S. Pope[5]
NASA Langley Research Center, Hampton, VA, 23681

One approach toward achieving NASA's aggressive N+2 noise goal of 42 EPNdB cumulative margin below Stage 4 is through the use of novel vehicle configurations like the Hybrid Wing Body (HWB). Jet noise measurements from an HWB acoustic test in NASA Langley's 14- by 22-Foot Subsonic Tunnel are described. Two dual-stream, heated Compact Jet Engine Simulator (CJES) units are mounted underneath the inverted HWB model on a traversable support to permit measurement of varying levels of shielding provided by the fuselage. Both an axisymmetric and low noise chevron nozzle set are investigated in the context of shielding. The unshielded chevron nozzle set shows 1 to 2 dB of source noise reduction (relative to the unshielded axisymmetric nozzle set) with some penalties at higher frequencies. Shielding of the axisymmetric nozzles shows up to 6.5 dB of reduction at high frequency. The combination of shielding and low noise chevrons shows benefits beyond the expected additive benefits of the two, up to 10 dB, due to the effective migration of the jet source peak noise location upstream for increased shielding effectiveness. Jet noise source maps from phased array results processed with the Deconvolution Approach for the Mapping of Acoustic Sources (DAMAS) algorithm reinforce these observations.

Nomenclature

D	=	Fan nozzle exit diameter
f	=	Frequency
M	=	Mach number
NPR	=	Nozzle pressure ratio
NTR	=	Nozzle temperature ratio
P	=	Pressure
St	=	Strouhal number
T	=	Temperature
U	=	Mean axial jet velocity
w	=	Microphone weighting term
x	=	Axial coordinate

Greek

α	=	Angle of attack
ϕ	=	Azimuthal angle
θ	=	Polar angle

Subscript

core	=	core stream quantity
fan	=	fan (bypass) stream quantity

[1] Research Aerospace Engineer, Aeroacoustics Branch, Mail Stop 461, Senior Member AIAA.
[2] Senior Research Scientist, Aeroacoustics Branch, Mail Stop 461, Fellow AIAA.
[3] Senior Research Engineer, Aeroacoustics Branch, Mail Stop 461, Senior Member AIAA.
[4] Research Aerospace Engineer, Aeroacoustics Branch, Mail Stop 461, Member AIAA.
[5] Senior Scientist, Analytical Services and Materials, Mail Stop 461.

m = microphone number
mix = mixed stream jet quantity
wt = wind tunnel quantity

I. Introduction

Aircraft noise continues to be an annoyance to communities near airports, an economic concern to airline operations, and an inhibitor to future growth of the aerospace market. Continued aircraft noise reduction through the introduction of new technologies is an important goal of the aeroacoustics community. The Environmentally Responsible Aviation (ERA) Project within NASA's Integrated Systems Research Program has been focused on near-term innovations for the simultaneous reduction of noise, emissions, and fuel burn. Toward that end, ERA adopted the N+2 Subsonic Transportation System Level Metric in 2009[1] which includes a system level aircraft certification noise goal of 42 cumulative EPNdB below Stage 4 for a large twin aisle aircraft. The timeframe for this goal is the demonstration of key technologies by the year 2020.

The aggressive N+2 noise goal, coupled with similar aggressive goals for emissions and fuel burn, warrants consideration of system level solutions beyond conventional tube-and-wing aircraft. The Hybrid Wing Body (HWB) aircraft is one such configuration that combines the aerodynamic benefits of a flying wing design with acoustic shielding of engines over the wing. More specifically, the HWB N2A-EXTE design shown in Fig. 1 is the result of a NASA Research Announcement (NRA) that began in 2008 with Boeing Research and Technology (NASA Contract Number NNL07AA54C). Additional industry and university team members included United Technology Research Center, the Massachusetts Institute of Technology (MIT), and the University of California Irvine (UCI). The culmination of this NRA was the delivery of a 5.8% scale model of the final N2A-EXTE design for aerodynamic and acoustic testing in NASA Langley's 14- by 22-Foot Subsonic Tunnel (hereafter referred to as the "14x22 Tunnel"). The purpose of the acoustic test was to provide high quality system level noise data to assess progress toward the 42 EPNdB ERA noise goal as well as to provide databases of component noise sources including spectra, levels, and directivities. These data will support the development and validation of new prediction capabilities within NASA's Aircraft NOise Prediction Program 2 (ANOPP2)[2] to more accurately predict noise from future unconventional aircraft configurations. The acoustic test was comprised of three main component investigations: turbomachinery noise, airframe noise, and jet noise, the last of which is the focus of this paper. Before discussing the test in more detail, it is important to mention two important components integral to the jet noise portion of the test – the jet rig and the nozzle system.

In order to accurately simulate jet noise within the 14x22 Tunnel, two Compact Jet Engine Simulator (CJES) units were designed, fabricated, and tested prior to the 14x22 Tunnel entry. These modular dual-stream, heated jet simulators were placed in close proximity to the three-dimensional airframe surface. A very compact design was required to minimize interference, maintain scale, and maximize capability for movement with respect to the model. Furthermore, minimizing rig noise, which can be prevalent for such a compact design, was an important requirement. Recent investigations[3-4] document the efforts behind the design and qualification of the CJES units prior to the HWB acoustic test.

The acoustic implications of an HWB-type design[5] include the use of propulsion airframe aeroacoustic installation effects such as shielding of engine sources with the fuselage to reduce far-field radiated noise. However, the jet noise source is distributed in nature and known to extend several diameters downstream of the nozzle exit. Therefore, effective shielding would require either placement of the engines unrealistically far upstream on the upper surface of the fuselage or technology to alter the jet noise source distribution so that shielding of jet noise can be effective at more realistic aft engine placements. The latter method has been the focus of several recent studies[6-8] that have led to the low noise nozzle design used in the current experiments.

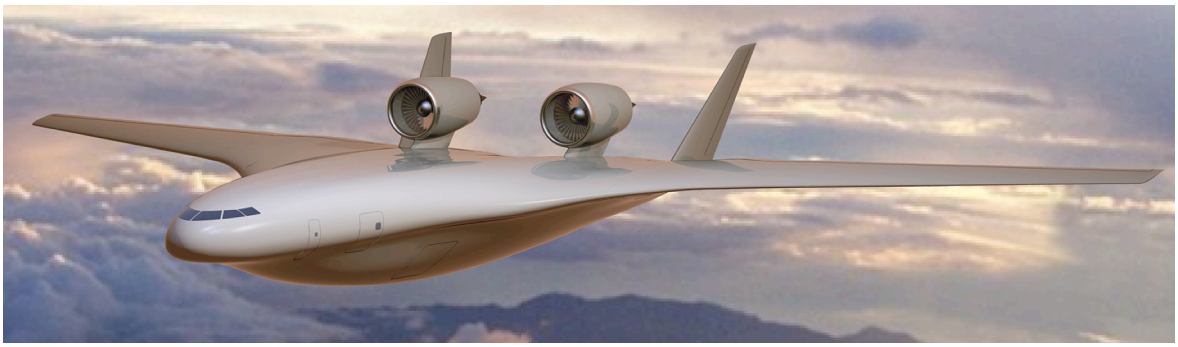

Figure 1. Artist rendering of the HWB N2A-EXTE aircraft concept designed by Boeing Research and Technology.

The CJES jet rig and low noise nozzle system were not the only systems developed to support the HWB acoustic test. Because heated jet experiments had not previously been performed within the 14x22 Tunnel, the implementation of an entire propane delivery infrastructure was required prior to testing. A traversing microphone phased array and microphones mounted on side towers and an overhead truss were also implemented for acoustic measurements. An associated high speed synchronous data acquisition system also had to be developed and interfaced with the existing wind tunnel systems. Heath *et al.*[9,10] describes in greater detail the preparations and facility upgrades required to support the HWB acoustic test. While the current paper describes the jet noise investigations, colleagues involved in other aspects of the test will be providing companion papers describing the microphone phased array development[11], acoustic calibration procedures[12], acoustic data processing[13], shielding characteristics of a mode generating source[14], shielding of broadband turbomachinery noise[15] and community noise metrics[16].

The current study provides an overview of the jet noise portion of the HWB acoustic test and focuses on the shielding benefits observed in conjunction with both the baseline axisymmetric nozzle system and the low noise nozzle system as the engines are translated relative to the fuselage trailing edge. Acoustic results from both the tower/truss arrangement and the overhead phased array are presented in this work. The next section of this paper discusses the tunnel facility, the HWB model, the CJES test rig, the instrumentation, and the data acquisition and processing. Section III examines the experimental results including the measured noise levels for each of the three community noise certification settings, effects of the CJES nozzle system, and effects of fuselage shielding on jet noise. Lastly, Section IV concludes with a summary of the results of the study.

II. Experimental Procedures

A. Facility

The HWB acoustic test took place in the 14x22 Tunnel[17] at NASA Langley Research Center. The tunnel is a closed-circuit, single return wind tunnel run at atmospheric pressure and powered with a 12,000 hp drive capable of speeds up to Mach 0.3. The closed test section measures 14.5 ft high by 21.75 ft wide by 50 ft long and can be configured in a closed or open configuration. This test was run with the test section in the open configuration with acoustic treatment on the floor, walls, ceiling, and model test stand as shown in Fig. 2. As noted in Heath *et al.*[9],

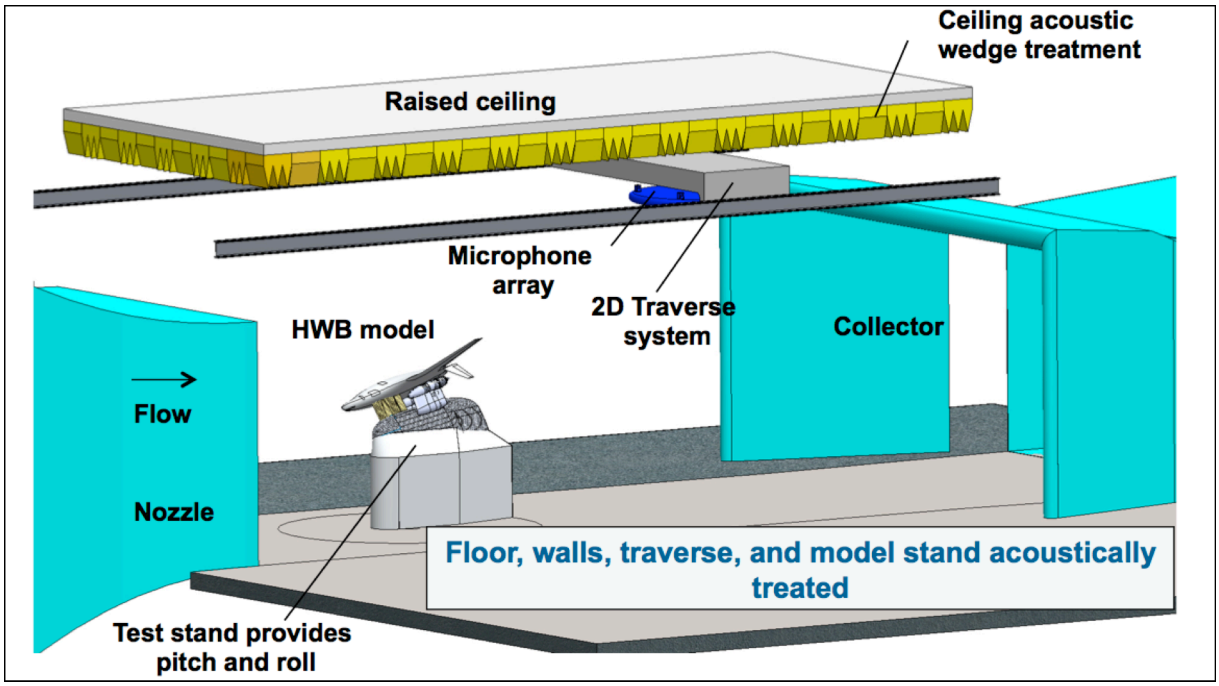

Figure 2. NASA Langley 14x22 Tunnel in acoustically-treated open test section configuration.

numerous facility enhancements to the 14x22 Tunnel were made in preparation for this acoustic test. The two most notable improvements were the addition of a traversing system for overhead phased array measurements and the fabrication of a fuel delivery system for supply of gaseous propane to the jet engine simulators for high temperature jet operations.

B. Hybrid Wing Body Model

The HWB wind tunnel model represents Boeing Research and Technology's Quiet R1 configuration, designated N2A-EXTE and is a 5.8% scale model with a length of 8.35 ft and a wingspan of 12.35 ft. The model shown in Fig. 3 has the capability to incorporate various vertical tail components, elevon deflections, leading edge components, and landing gear assemblies. The model is equipped with 248 surface pressure taps for aerodynamic investigations, four temperature sensors aft of the nacelle locations for surface temperature monitoring during heated jet testing, and six speaker drivers for position verification during microphone phased array processing. Flow-through nacelles are mounted on top of the fuselage for conventional aerodynamic testing. For acoustic testing, the model is inverted, and either the Broadband Engine Noise Simulators (BENS) used for simulating turbomachinery noise[15] or the CJES units used for simulating jet noise can be mounted underneath the model on the acoustic model support stand as observed in Fig. 4. Both sets of simulators are capable of translating in the axial direction independent of the fuselage body so that the extent of shielding can be varied at discrete axial stations from x/D = -0.5 to x/D = 3.0 where D is the fan nozzle exit diameter and x is the axial distance from the fan nozzle exit plane to the model trailing edge at the jet centerline. Positive values of x represent a fan nozzle exit location upstream of the model trailing edge. The x/D = 2.5 position is the baseline or design location of the HWB engines to take advantage of shielding. Conversely, moving the engines to the full aft position of x/D = -0.5 represents an unshielded configuration.

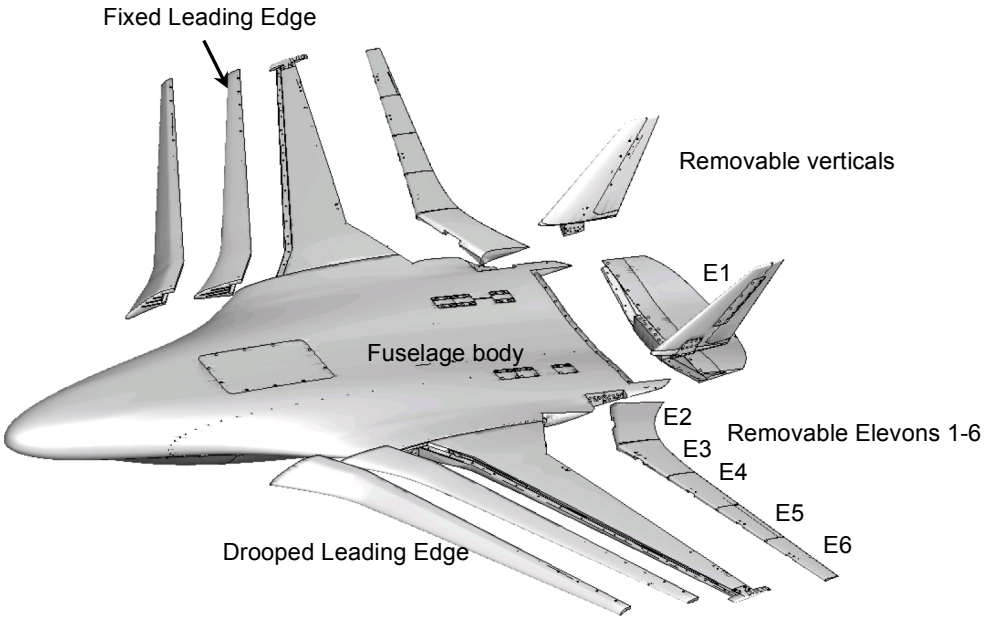

Figure 3. HWB wind tunnel model with modular components, 5.8% scale.

C. CJES Units

A schematic of a single CJES unit is shown in Fig. 5a. Each unit is configured for a bypass ratio 10 cycle, to deliver up to approximately 8 lbm/s of fan stream airflow at temperatures up to 150° F and almost 1 lbm/s of core stream airflow at temperatures up to 1500° F. Air is supplied through two-inch flexible rubber hoses for each stream. Figure 5b shows the charging station that consists of two temperature rakes of 4 thermocouples each for the core stream and 5 thermocouples each for the fan stream. Likewise, two total pressure rakes of 4 ports each for the core stream and 5 ports each for the fan stream are included, with an additional port at the tip of the charging station centerbody. In total, 19 total pressure ports and 18 total temperature probes are contained in the CJES charging station, as well as two static pressure ports in each of the core and fan streams. The outputs of these total probes were averaged together for use in determining nozzle pressure ratio (NPR) and nozzle temperature ratio (NTR).

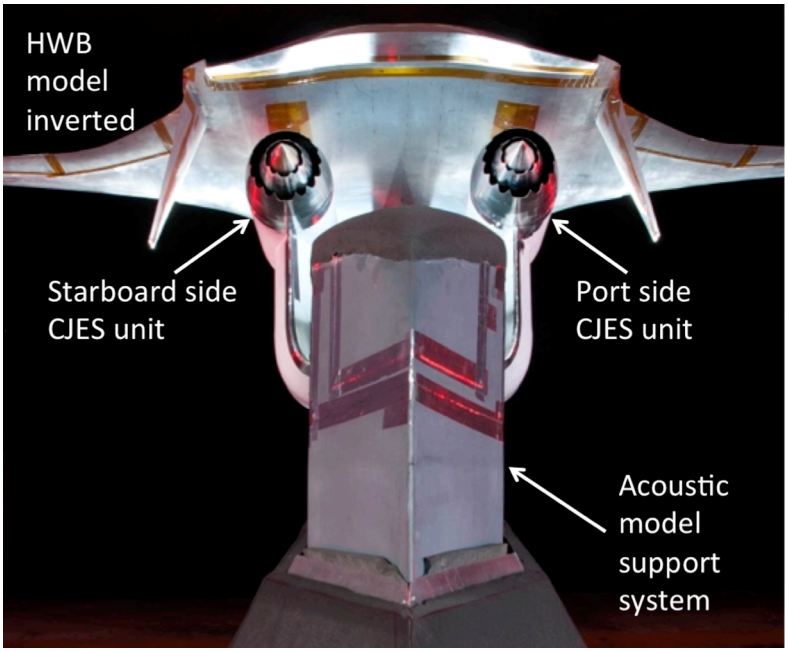

Figure 4. Compact Jet Engine Simulator (CJES) units mounted underneath the inverted HWB model .

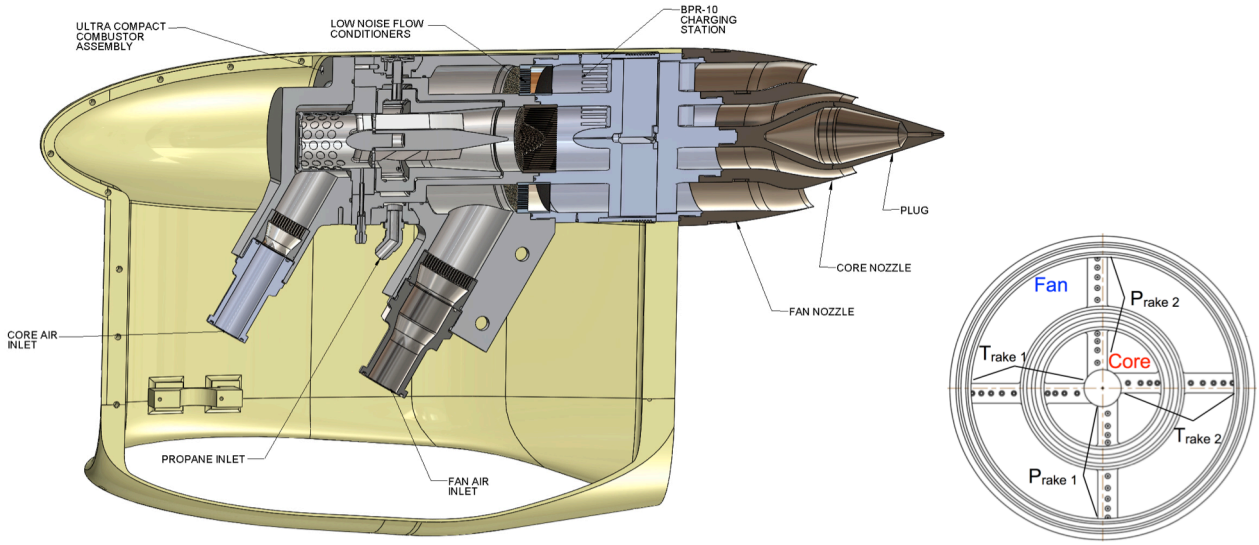

a) **b)**

Figure 5. Schematic of a) CJES unit and b) charging station.

The fuel delivery system for the CJES units includes a vaporizer for conversion of liquid propane to gaseous propane. A nitrogen-purged containment vessel for each CJES unit also encases all fuel delivery control valves to ensure safe operation under the 14x22 Tunnel floor. A 0.5" flexible rubber hose supplies the gaseous propane to the CJES unit where it is injected through six fuel injectors mounted in separate circumferential flame-holder grooves recessed around the outer diameter of the swirl air cavity of an Ultra Compact Combustor (UCC). The fuel mixes with the swirl air injected through 24 ports angled at 45° around the cavity. The mixture is ignited by a single ceramic igniter that can be turned off once the mixture is burning.

The use of UCC technology adapted from Zelina *et al.*[18] was an important component of the CJES development. The UCC uses centrifugal loading to reduce combustion volume and thus reduce the overall length of the engine simulators. Nonetheless, the combustion and rig noise challenges that accompany such small jet engine simulators require careful attention to the selection and placement of flow conditioners within the CJES units as further described in previous work[4].

Two sets of convergent core and fan nozzles are available for testing with each CJES unit – one set is axisymmetric while the other set includes an essentially uniform core chevron nozzle and an asymmetric fan chevron nozzle. The axisymmetric nozzle set provides a useful database of a conventional nozzle system applied to the HWB configuration. Furthermore, it provides a baseline by which to assess the performance of the low noise chevron nozzle set. The low noise nozzle set is necessary to reduce the jet noise contribution of the system level noise toward the 42 EPNdB goal. The chevron nozzles were designed based on extensive testing described by Thomas *et al.*[8] A separate plug for the core stream also accompanies each set of nozzles. To maintain constant thrust, the chevron nozzle exit areas were made approximately 2% larger than the corresponding axisymmetric nozzle exit areas by altering the plug and core nozzle outer contour lines. For both the axisymmetric and chevron nozzle sets, the core nozzle exit diameter is 3.28 inches and the fan nozzle exit diameter is 6.21 inches.

D. Instrumentation

1. Tower/Truss Microphones

An azimuthal array of 29 Brüel and Kjær (B&K) Type 4138 pressure field microphones of 0.125" diameter were mounted around the test section outside of the wind tunnel shear layer on two sideline towers and an overhead traverse truss as shown in Fig. 6. These microphones, 8 on each sideline tower and 13 on the overhead truss, were positioned perpendicular to the flow with grid caps removed and spaced at approximately 7.5° increments azimuthally. The closest radial distance from the microphones to the CJES centerline was approximately 153.5 inches and occurred when the center truss microphone was over the model. The microphones could be traversed axially in concert to capture a significant portion of the polar and azimuthal acoustic directivity pattern of

the HWB with operating CJES units. Typically, tower/truss microphone data were acquired at nine axial stations along a 23.5 ft axial distance fore and aft of the model. Initial microphone locations were identified with laser measurements and maintained with the traverse encoder on the linear rail system. However, a photogrammetry system was also employed to ensure accurate positioning of instrumentation within the test section. Tower/truss microphones were used with ⅛" to ¼" adapters to attach to Model 2670 pre-amplifiers, powered by B&K Model 5135L two-channel power supplies. Pistonphone calibrations were performed before and after the test and typically weekly during the test. Injection calibrations were also periodically performed by applying a white noise signal with known RMS voltage to each preamplifier and recording the output signal.

2. Microphone Phased Array

In addition to the tower/truss microphone system, a two-dimensional phased array system was used for identification and quantification of noise source locations on or near the model system. An array of 97 B&K Model 4938 pressure field microphones of 0.25-inch diameter were surface-mounted in an 8.05 ft disc on the same overhead traverse system used for the truss microphones shown in Fig. 6. Note that the phased array disc was located in the same vertical plane as the truss microphones, but with its center approximately 62 inches upstream of the truss microphones. The array has a maximum aperture size of 78.6" with a solid angle of 29.4° at a 12.5 ft working distance. The array was designed for a frequency range of 1.5 kHz to 80 kHz using 16 array arms with 6 microphones in each arm and one additional center microphone. In addition to initial laser positioning and photogrammetry, a series of accelerometers and inclinometers were used to monitor the array panel position and vibration characteristics and thus ensure a favorable measurement environment during tunnel operations. Microphones were used in conjunction with Model 2670 preamplifiers, powered by Model 5935L two-channel power supplies (inner 48 microphones of array) and Model 2829 four-channel power supplies (remaining 49 microphones). Pistonphone calibrations were performed before and after testing while embedded speakers were utilized to perform in-situ calibrations during testing, and injection calibrations were also performed periodically.

E. Data Acquisition and Processing

The acoustic data acquisition system (DAS) supported 192 dynamic channels and consisted of a series of commercially available hardware from National Instruments and Precision Filters Inc. all coordinated through a LabVIEW master program. National Instruments PXI-6120 high speed digitizer cards were used in conjunction with a Precision Filters Inc. 28000 system for signal conditioning. The high and low pass filter settings were 400 Hz and 100 kHz, respectively. Data were sampled at 250 kHz and processed in blocks of 8192 samples, resulting in acoustic spectra consisting of 4096 points with a frequency resolution of 30.52 Hz. Typical acquisition times were approximately 30 seconds in length. The master program controlled not only the dynamic channel acquisition, but

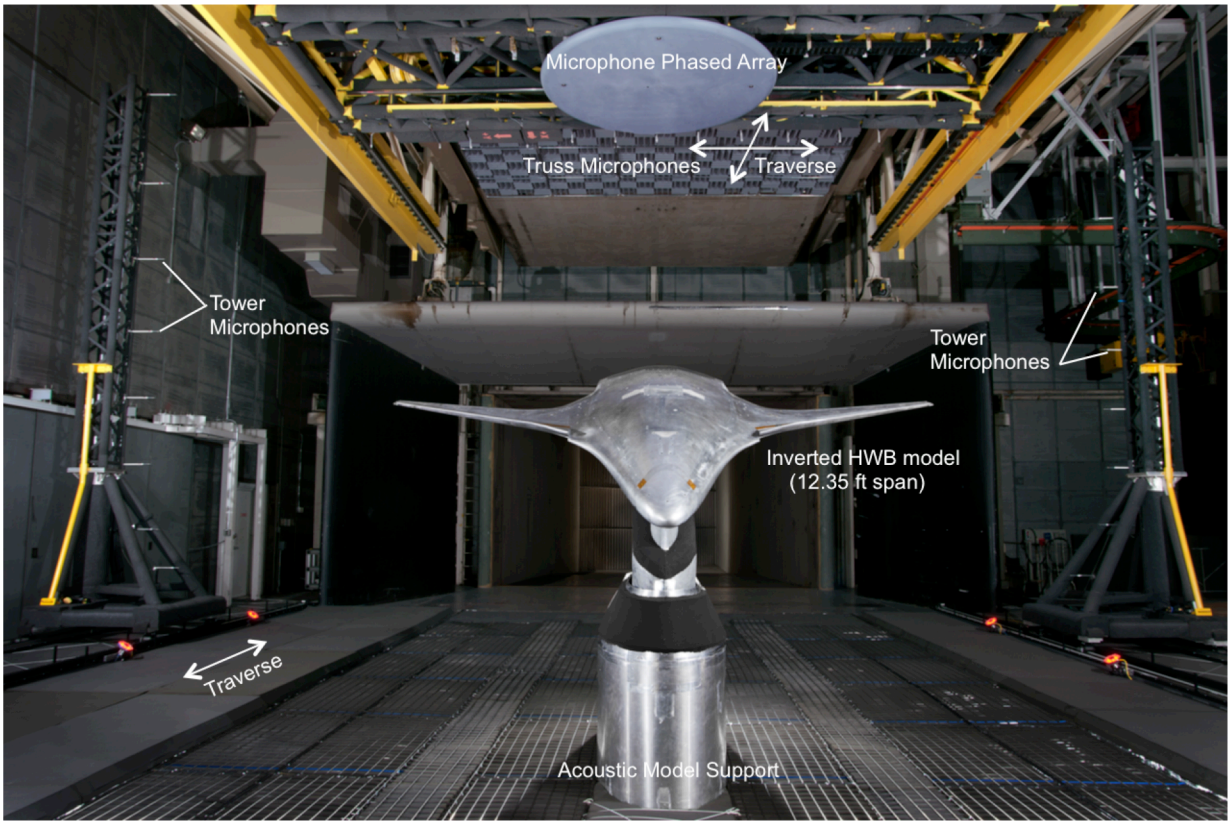

Figure 6. Microphone phased array and tower and truss microphone instrumentation in 14x22 Tunnel test section.

also the overhead traverse and tower rail system. Furthermore, the master program interfaced with the 14x22 Tunnel data system, the CJES data system, and the inclinometers on the phased array to simultaneously provide important information regarding the wind tunnel, the model, the CJES units and the phased array orientation. Therefore, high speed communication and proper synchronization were imperative, and further details are discussed in Heath *et al.*[10]

Processing of the acoustic data requires application of several corrections: rejection of contaminated time history data as needed (due predominantly to buffeting from the wind tunnel shear layer), microphone and filter frequency response corrections, background noise subtraction, shear layer corrections using Amiet's method[19], microphone directivity corrections, and atmospheric attenuation corrections to a lossless condition according to the ANSI standard[20]. The aforementioned corrections have been applied to all single microphone data associated with the tower/truss microphones unless otherwise noted. Microphone phased array data include similar corrections with the exception of the microphone directivity correction which has not been applied. The phased array data also go through an additional processing algorithm incorporating the Deconvolution Approach for the Mapping of Acoustic Sources (DAMAS)[21]. DAMAS is applied to remove the array characteristics from the noise source map results. As part of the deconvolution, techniques such as diagonal removal to reduce the impact of microphone self noise and microphone weighting to maintain beamform resolution over a range of frequencies are also employed in the current work. However, unlike Brooks *et al.*[22], there is no cross spectral matrix conditioning performed in the current analysis. Lastly, a series of 256 DAMAS iterations are used throughout the current work.

III. Experimental Results

A. Flow Conditions

The flow conditions examined in this work focus on the approach, cutback, and takeoff (sideline) bypass ratio 10 cycle points of the HWB that are simulated using the dual stream CJES units. Table 1 describes these flow conditions in more detail. Although multiple wind tunnel Mach numbers were investigated for the cutback and takeoff conditions, the background noise levels for the M_{wt} = 0.23 cases were typically too high for accurate measurements at low frequencies. Thus, the focus will be on the M_{wt} = 0.17 cases for all setpoints.

Table 1. Experimental conditions, characteristic frequency (f_c) calculated assuming standard day.

NPR_{core}	NTR_{core}	NPR_{fan}	NTR_{fan}	M_{wt}	$f_c = U_{mix}/D_{mix}$ (Hz)	α	*HWB Cycle point*
1.034	2.088	1.117	1.037	0.17	1139	13.2°	Approach
1.240	2.721	1.461	1.124	0.17, 0.23	2219	14.5°	Cutback
1.411	2.956	1.607	1.161	0.17, 0.23	2555	15.5°	Takeoff

B. Data Comparison

The quality of acoustic data from this test is discussed in works by Spalt *et al*[12] and Bahr *et al*[13] as they discuss facility calibration of the 14x22 Tunnel and data processing, respectively. Another quality check, specifically applicable to the CJES data analysis, is a jet spectral comparison to other relevant acoustic data. The closest relevant data available for comparison is from Boeing's Low Speed Aeroacoustic Facility (LSAF) of an isolated jet exhaust obtained during the investigation described in Thomas *et al*[8]. Figure 7 shows a narrowband spectral comparison at θ=145° (and ϕ = 0°) of the axisymmetric nozzle set for the unshielded axial position in the 14x22 Tunnel compared to a scenario in which no airframe model was present in LSAF . In both cases data were corrected according to the process mentioned in Section 2E. In addition, slight scale adjustments were taken into account (6.2% scale in LSAF vs. 5.8% scale in 14x22), and the LSAF data were corrected to the distance of the 14x22 truss microphone. Lastly, frequencies were nondimensionalized to Strouhal number based on mixed jet velocities and equivalent mixed flow jet diameters for each case:

$$St = \frac{f}{(U_{mix}/D_{mix})}. \tag{1}$$

Spectral levels were correspondingly adjusted to 1 Hz common bandwidth and to a per unit Strouhal number basis for consistency with the frequency nondimensionalization according to

$$SPL\ (dB\ per\ unit\ St\#) = SPL + 10\log_{10}\left(\frac{U_{mix}/D_{mix}}{\Delta f}\right). \tag{2}$$

Figure 7 shows that while the spectral shape compares favorably between facilities for this case, the LSAF data has a slightly lower amplitude by 1.5 to 2.0 dB. This is not surprising, given that the 14x22 Tunnel spectrum also includes the full HWB model and CJES units at 14.5° angle of attack.

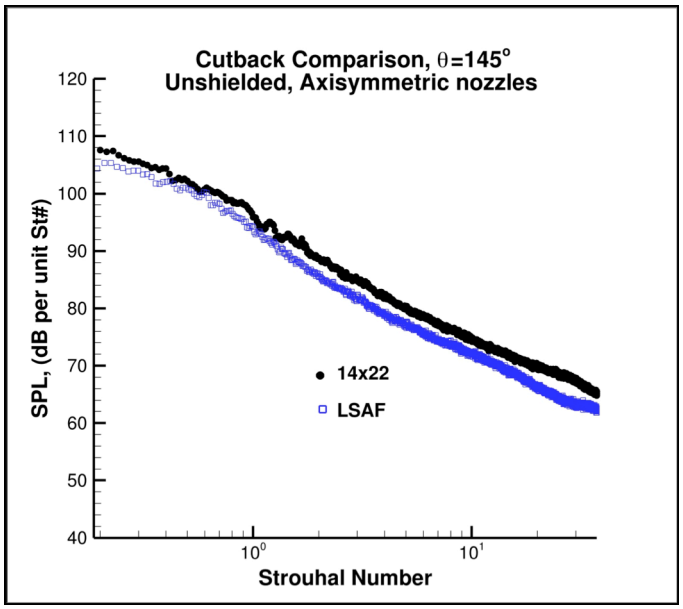

Figure 7. Narrowband spectral comparison between port CJES operating in 14x22 and isolated jet in LSAF operating at nominal cutback condition: (14x22: NPR_{core} = 1.24, NPR_{fan} = 1.461, NTR_{core} = 2.721, NTR_{fan} = 1.124, M_{wt} = 0.17 and LSAF: NPR_{core} = 1.28, NPR_{fan} = 1.506, NTR_{core} = 2.784, NTR_{fan} = 1.134, M_{wt} = 0.17).

C. Tower/Truss Microphone Measurements

In addition to utilizing single microphone spectral measurements, the tower and truss microphones can be analyzed as a system providing valuable information about the directivity characteristics of the system configurations investigated.

1. Noise Hemispheres

As the tower/truss microphones are traversed axially, around and over the inverted HWB model, contours of corrected sound pressure level (SPL) are created along a three-sided surface that resembles a row of staples as shown in Fig. 8a. Each dot in Fig. 8a represents the location of a microphone measurement with interpolation occurring between these locations. This "staple" plot is then converted to a noise hemisphere as shown in Fig. 8b. The hemisphere uses emission coordinates, has a 15 ft radius, and is centered at the core nozzle exit plane along the jet centerline of the operating CJES unit or on the midpoint between jet centerlines if both units are operating. Next, the hemisphere is rotated such that the HWB is right side up and the observer is toward the ground as shown in Fig. 8c. The coordinate axes are fixed at the center of the hemisphere (nozzle exit plane) with polar angle θ defined relative to the longitudinal axis of the aircraft with $\theta = 0°$ at the nose and $\theta = 180°$ at the jet axis. Azimuthal angle ϕ is defined laterally across the aircraft with $\phi = 0°$ directly underneath the aircraft centerline and negative values of ϕ occuring under the port side of the aircraft. Because the CJES units can be translated axially independent of the HWB model, the origin of this coordinate system changes slightly with configuration. Lastly, the hemisphere is propagated to a 100 ft radius and flattened out onto a two dimensional plot with θ along the x-axis and ϕ along the y-axis, as shown in Fig. 8d. In this plot, flow is from left to right, and the port side of the aircraft is at the bottom of the plot. The noise source is centered at $\theta = 90°$ and $\phi = 0°$. While this plotting format is just one way to visualize these data, it is particularly conducive to community noise predictions using ANOPP2. Data presented in the next section are an example of the basis of such a noise prediction.

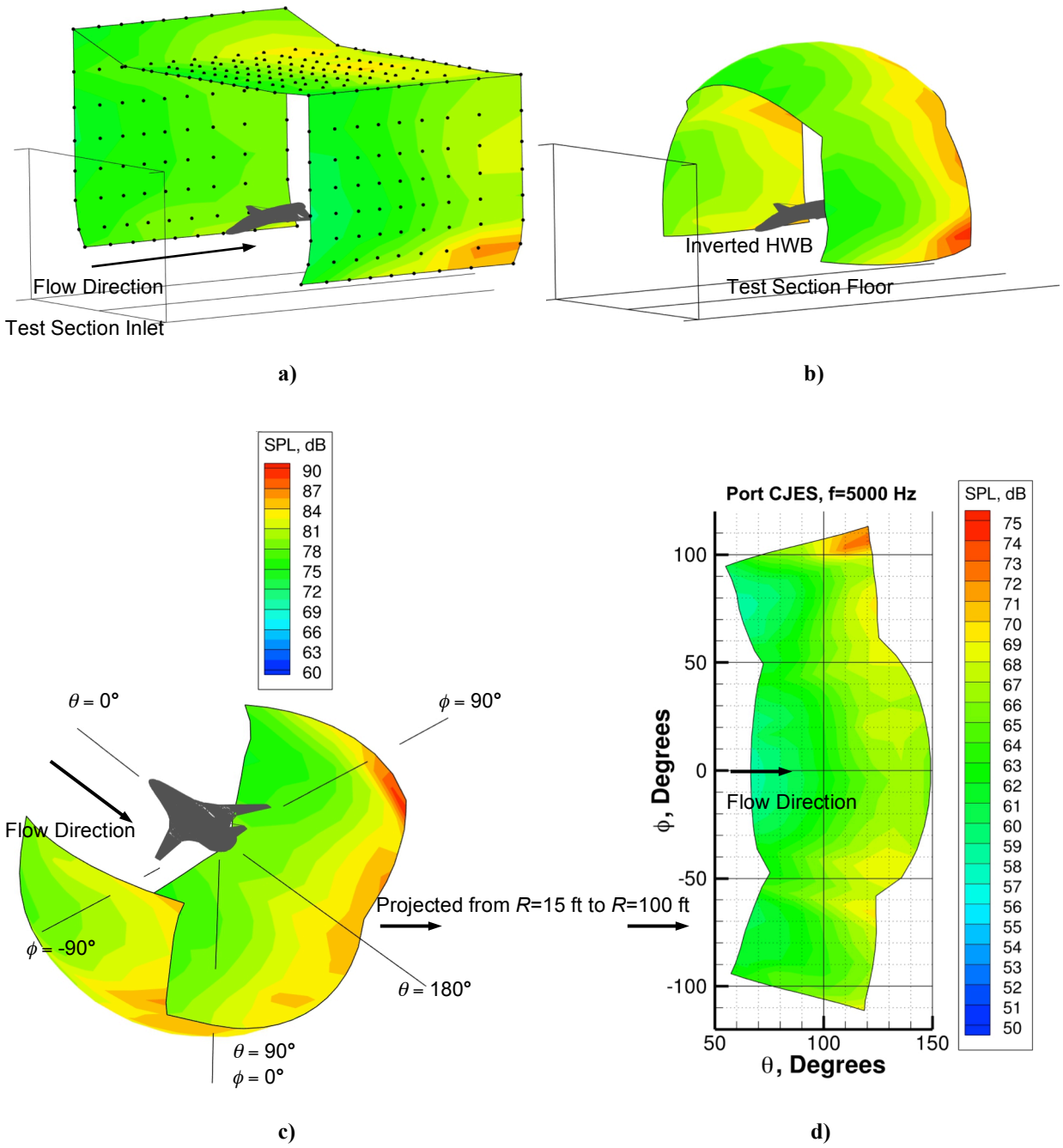

Figure 8. Tower/Truss microphone results are used to generate noise hemispheres according to the steps shown: a) Original staple plot of corrected sound pressure levels, b) Noise hemisphere at 15 ft radius from CJES nozzle exit plane, c) Inverted hemisphere so HWB in correct orientation, and d) Hemisphere projected to 100 ft radius and flattened into two-dimensional contour. Case shown is for port CJES operating at cutback cycle conditions with M_{wt} = 0.17.

2. CJES Noise Levels for HWB Community Noise Assessment

As previously mentioned in Section 1, one of the goals of the current HWB test is to provide system level noise data for use in assessing the capability for this HWB design to achieve the 42 cumulative EPNdB below Stage 4 flight certification noise goal. Figure 9 shows the noise hemispheres at the three noise certification points – approach, cutback, and takeoff (sideline) for the 5000 Hz model scale one-third-octave band. The range of model scale frequencies presented in this work, 5000 Hz to 20000 Hz, corresponds to a full scale frequency range of 290 to 1160 Hz. These data correspond to the low noise engine design configuration in that the chevron nozzles are installed and the engines are in the x/D = 2.5 shielded configuration as shown in the model image above the contours. The HWB model is shown with the CJES units which require additional upstream length for plumbing (shown in blue) that would not be present on the actual flight vehicle. All of the cases shown here, and throughout this work unless otherwise noted, make use of the HWB model in its baseline aerodynamic configuration. That is, with wing leading edge droop, baseline narrow twin vertical tails with 10° outward cant and an aft mounted location, center elevon deflected -10° (toward engines), all other elevons at 0°, and angle of attack settings corresponding to those listed in Table 1 for each cycle point.

For the approach case of Fig. 9a both CJES units were operating, while for the cutback and takeoff cases, the port or starboard CJES units were operated individually as is noted above the contour plots throughout the paper. Not surprisingly, the approach noise levels are significantly lower than those observed for cutback and takeoff. Due to a mismatch of desired and actual fan stream nozzle pressure ratio discovered after testing for the particular run associated with Fig. 9c, the takeoff cycle point was significantly lower than expected. Thus, a factor of 4.55 dB has been added to the data shown in Fig. 9c based on the scaling of mixed jet velocity to the eighth power: 80 $\log_{10}$ ($U_{mix\ desired}/U_{mix\ actual}$). The contours in Fig. 9 undergo additional scaling and extrapolation as detailed in Burley *et al.*[16] to generate the expected jet noise contribution to the HWB community noise assessment.

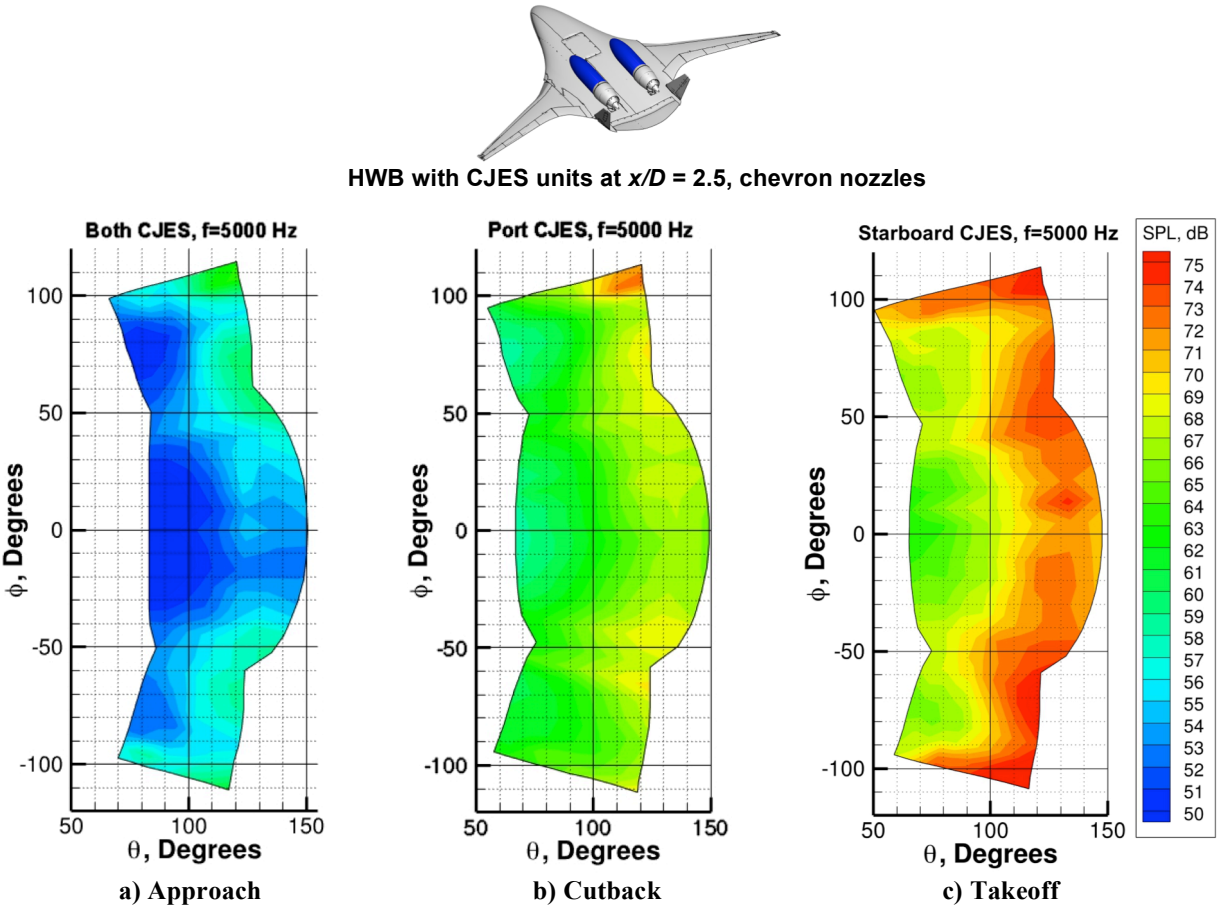

Figure 9. Theta-Phi noise hemispheres for f = 5000 Hz one-third-octave band for shielded jet operating at x/D = 2.5 with chevron nozzle set at a) Approach b) Cutback, and c) Takeoff cycle conditions, M_{wt} = 0.17.

3. CJES Nozzle System Effects

The acoustic performance of the low noise chevron nozzle set was compared to the performance of the axisymmetric nozzle set in the unshielded engine configuration. While careful chevron designs can reduce the overall jet source strength, the work of Thomas *et al*.[8] focused on a design that would both reduce source strength and increase shielding effectiveness by moving peak jet noise source locations further upstream for the distributed source. The first of these goals is now addressed, with the second goal of influencing the peak source location left to the upcoming phased array discussion.

Figure 10 shows a set of ΔdB contours between the unshielded (x/D = -0.5) chevron nozzle set and the unshielded baseline nozzle set at cutback conditions for three different one-third-octave model scale frequencies. Figure 10a shows reduction of jet noise at 5000 Hz on the order of 1 to 2 dB across the contour. At 10,000 Hz the benefit is about 0.5 to 1.0 dB in the downstream direction but there is a penalty in the upstream direction ($\theta < 90°$), as seen in Fig. 10b. In Fig. 10c at 20,000 Hz, a more substantial penalty of 1 to 2 dB at the upstream locations is noted. Although the high frequency increases might seem unacceptable at first glance, the design intent was to maximize the benefit for a shielded configuration in which much of the near nozzle high frequency penalty can be effectively shielded. These trends and levels are very similar to those shown in Figure 10 of Thomas *et al.*[8], thus further confirming those results. Finally, the increases at the upper and lower edges of the contour of Fig. 10c occur where $\phi > 90°$ as the observer is transitioning to the upper half plane of the nozzle system. With its asymmetric chevrons, the fan nozzle is designed to optimize the noise reduction in the typical observer direction centered around $\phi = 0°$.

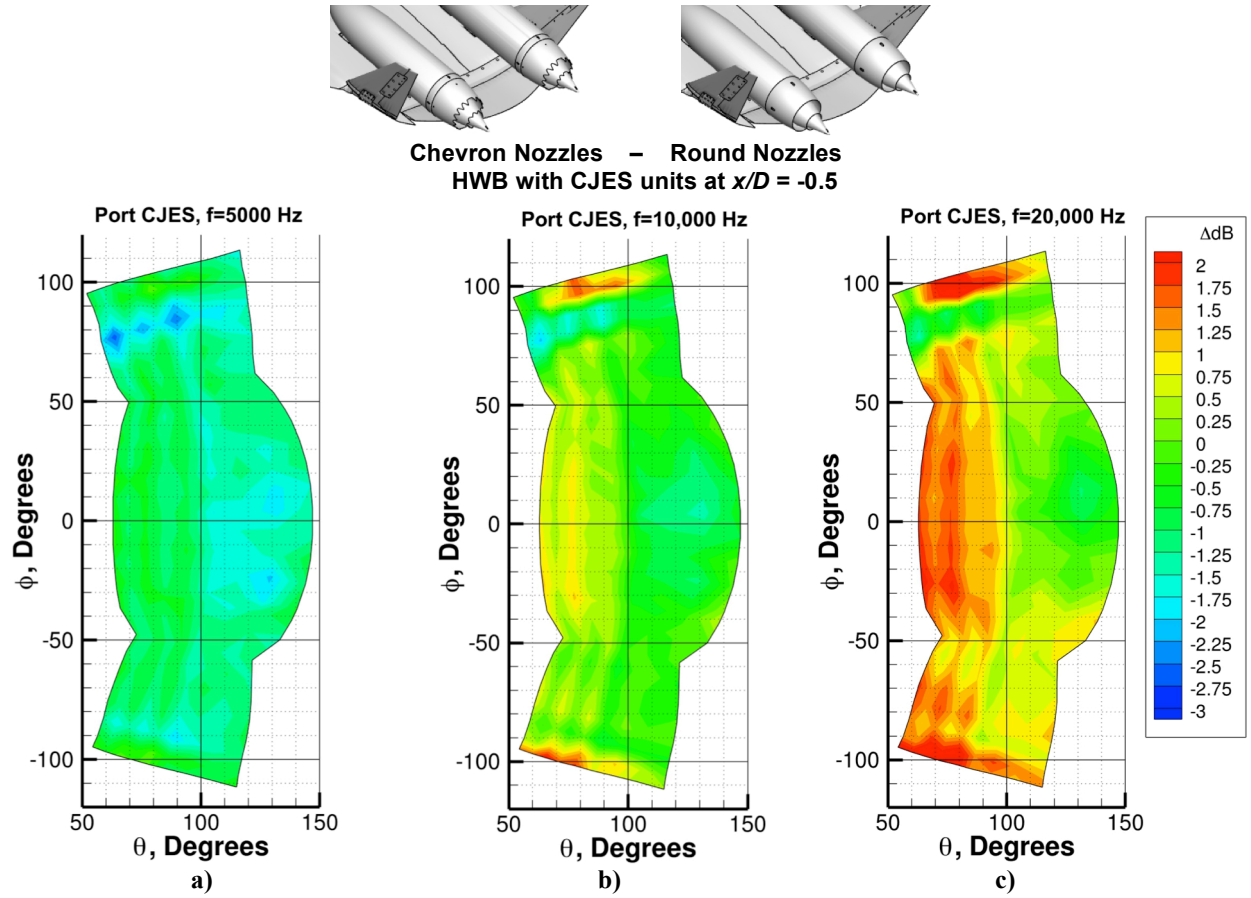

Figure 10. Theta-Phi hemispheres of ΔdB contours of chevron-round nozzle at x/D = -0.5, port CJES operating, cutback cycle conditions, M_{wt}=0.17, at three one-third-octave frequencies: a) 5000 Hz, b) 10,000 Hz, and c) 20,000 Hz.

4. Shielding Effects

Thus far, all comparisons of CJES noise levels have been with the engine simulators at consistent axial stations. Figure 11 shows the effect of moving the CJES units upstream with the axisymmetric round nozzle system at cutback conditions. A ΔdB contour showing the difference in noise level with the CJES units at the shielded design location (x/D = 2.5) compared to the unshielded location (x/D = -0.5) is shown for the same one-third-octave frequencies as Fig. 10. The 5000 Hz case of Fig. 11a shows shielding benefits of approximately 1 to 4 dB with higher benefits in the upstream direction. As expected, shielding becomes more effective at higher frequencies, as Fig. 11b demonstrates, with benefits of up to 5 dB from shielding. At the highest frequency of 20,000 Hz in Fig. 11c the shielding benefits are up to 6.5 dB with the most effective shielding occurring directly under the body and slightly downstream of it. Not only does shielding becomes less effective as the azimuthal angle increases toward ± 90°, but there are noticeable increased sound pressure levels measured at the highest azimuthal angles which represent the lowest microphones on each microphone tower. As the CJES units are moved further under the fuselage, sound can reflect toward these locations, which would be away from a ground observer. Higher levels appear more prevalent on the starboard (top) edge of the contour (at least in Figs. 11a and 11b.) This is quite possibly due to reflection of jet noise from the operating CJES on the port side, potentially involving the vertical tail.

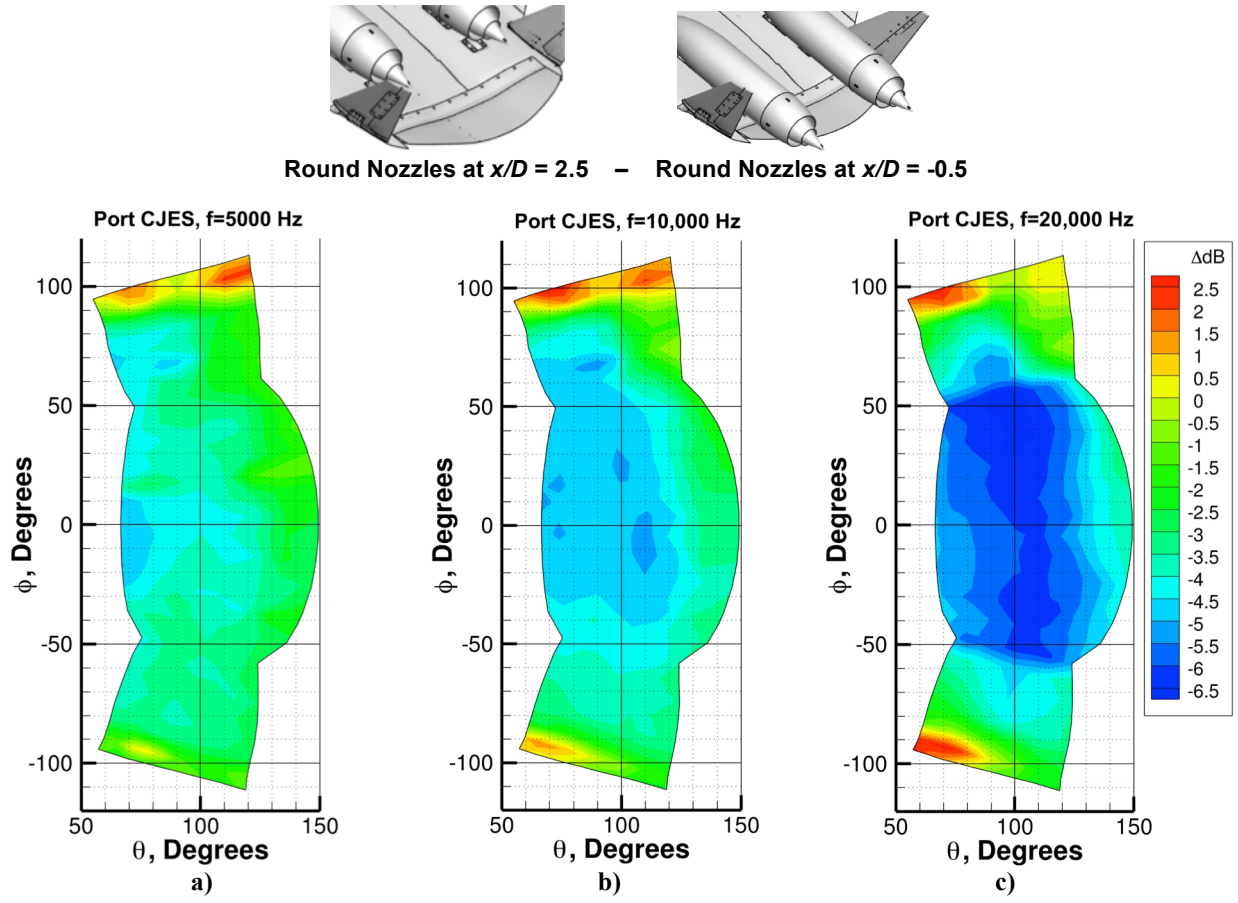

Figure 11. Theta-Phi hemispheres of ΔdB contours of shielded-unshielded round nozzle, port CJES operating, cutback cycle conditions, M_{wt} = 0.17, at three one-third-octave frequencies: a) 5000 Hz, b) 10,000 Hz, and c) 20,000Hz.

While Fig. 11 showed the shielding benefits using an axisymmetric nozzle system, Fig. 12 begins to address the effects of shielding with the chevron nozzle set. The noise contours of Fig. 12 show the effects of increased shielding at 5000 Hz in going from x/D = -0.5 (unshielded) in Fig. 12a, to x/D = 1.5 in Fig. 12b, to x/D = 2.5 (design location) in Fig. 12c. At the x/D = 2.5 location decreased noise levels in the upstream direction are becoming more distinct.

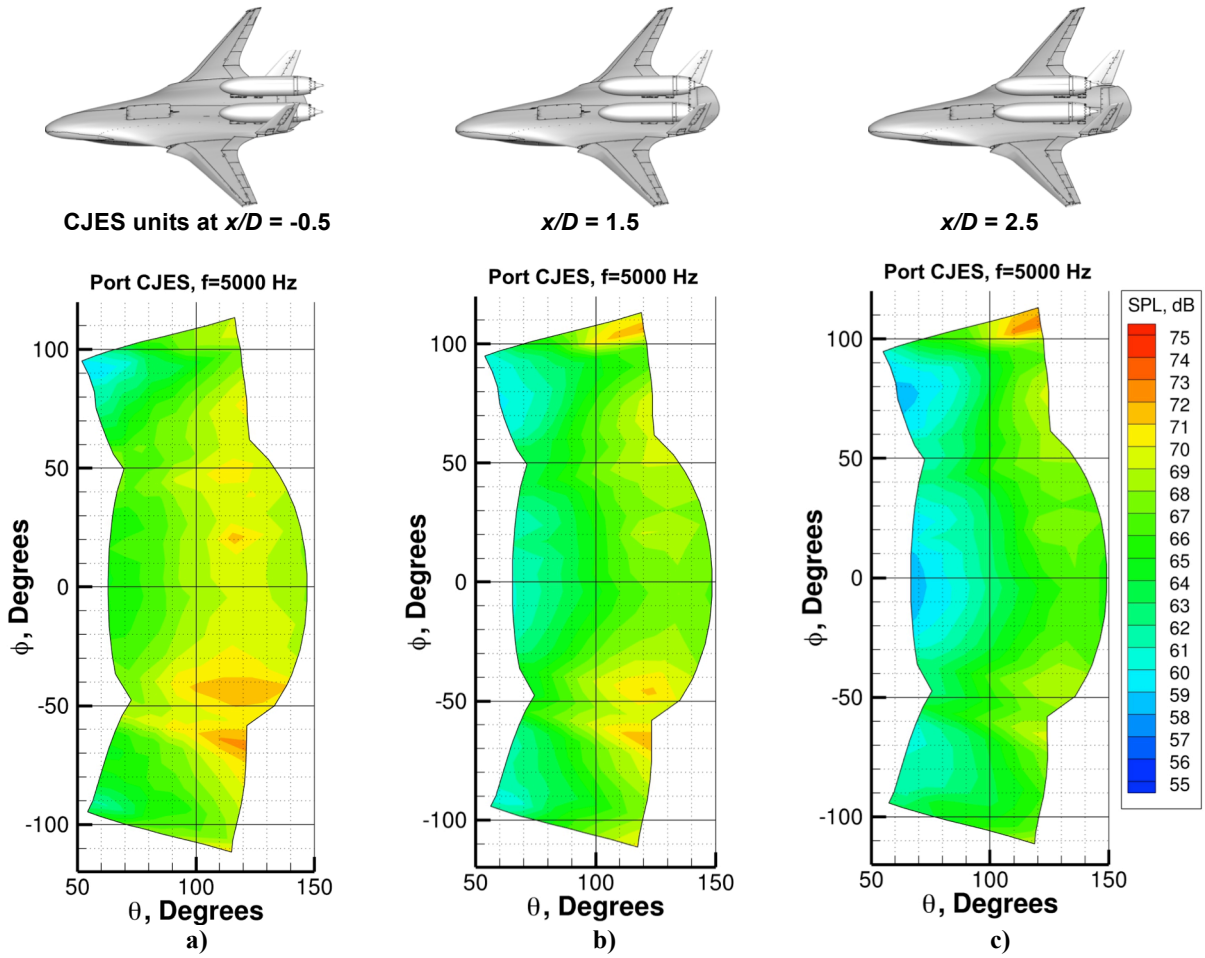

Figure 12. Theta-Phi noise hemispheres of f = 5000 Hz one-third-octave band showing the effect of increased shielding using the chevron nozzles at cutback conditions, port CJES operating, M_{wt} = 0.17 for a) x/D = -0.5 b) x/D = 1.5, and c) x/D = 2.5.

By subtracting the results of Fig. 12a from 12c, the ΔdB contour of Fig. 13 is produced. In addition, two other frequencies are included making Fig. 13 the chevron nozzle equivalent of Fig. 11. Note the increased legend limits in Fig. 13 relative to Fig. 11, indicating increased levels of shielding with the chevron nozzle set. Just as was found for the axisymmetric nozzle set, measurements for the chevron nozzle set also show increases in noise at large azimuthal angles, particularly on the starboard (top) of the contour where noise from the port CJES may be reflecting off the vertical tail. A noise benefit of up to 6.5 dB is noted for the 5000 Hz case of Fig. 13a. The behavior of the higher frequency cases is similar to those for the axisymmetric nozzle, albeit at increase levels of shielding. Figure 13b shows shielding benefits at 10,000 Hz to be as much as 9 dB in the upstream locations. Furthermore, at 20,000 Hz benefits are near 10 dB over approximately half of the contour region. If the chevron nozzle system only reduced the jet source strength, one might assume that the source strength reduction of Fig. 10 and the shielding benefit of Fig. 11 could be summed to predict the total benefit of the shielded chevron noise in Fig. 13. The fact that the actual benefits of Fig. 13 are greater than the sum of each effect suggests that the nozzle system is also increasing the shielding effectiveness by modifying the peak source location. The evidence of this change is more clearly shown in the microphone phased array results to follow.

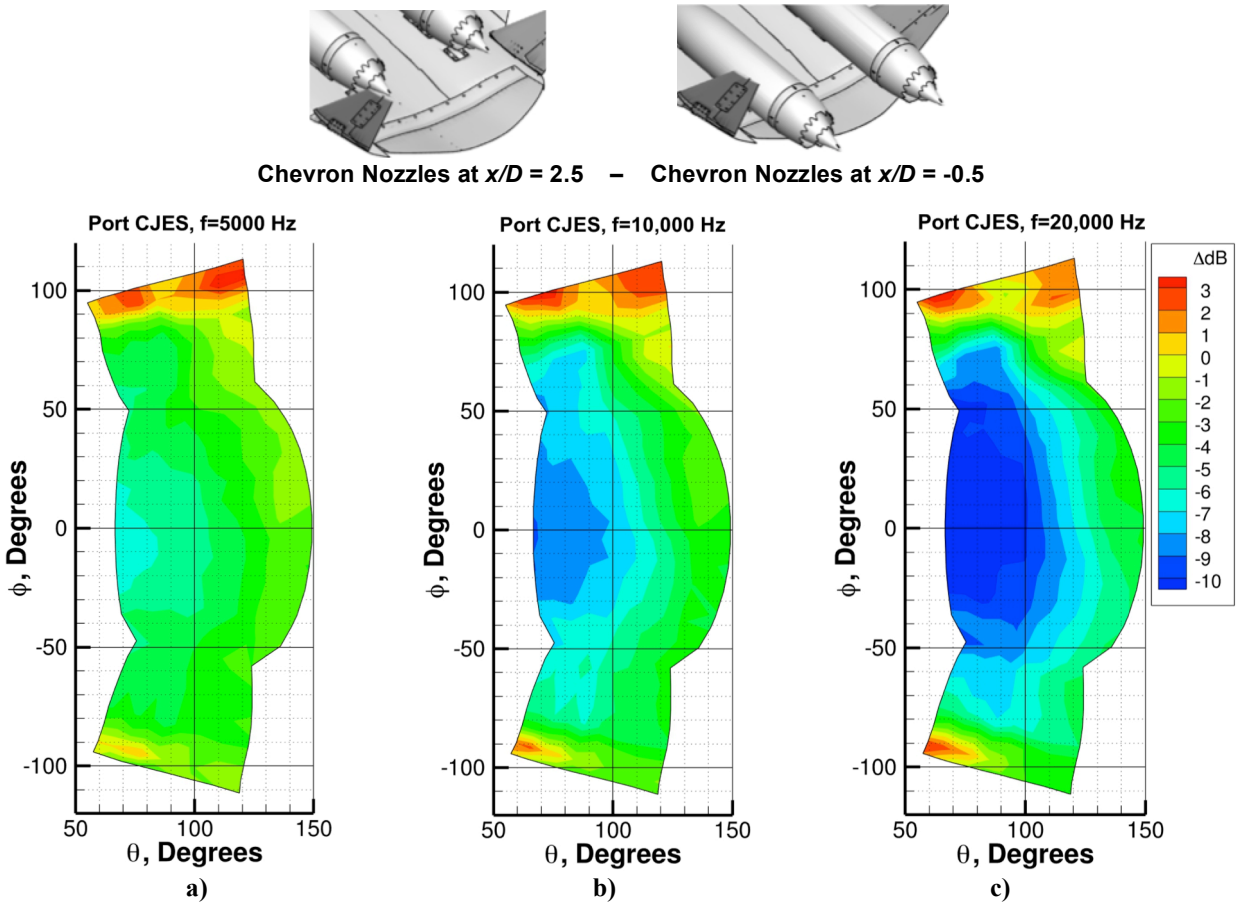

Figure 13. Theta-Phi hemispheres of ΔdB contours of shielded-unshielded chevron nozzle, port CJES operating, cutback cycle conditions, M_{wt} = 0.17, at three one-third-octave frequencies: a) 5000 Hz, b) 10,000 Hz, and c) 20,000Hz.

D. Microphone Phased Array Measurements

The CJES noise source field can be effectively mapped using the overhead phased array microphones and the DAMAS deconvolution array processing algorithm. A 1" by 1" resolution grid plane that is 100" wide by 140" long is used. The plane is parallel with the waterline of the model and is aligned with the model trailing edge. The result is a map of the dominant noise field in relation to the HWB and nozzle geometries. Such maps are extremely useful in understanding how the nozzle set and shielding location affect the noise source field. Figure 14 shows five maps generated using DAMAS for the f = 5000 Hz one-third-octave band: two axisymmetric nozzle set noise maps are shown on the left (Fig. 14a and d). Figure 14a is the unshielded case (x/D = -0.5), and Fig. 14d is the shielded case (x/D = 2.5). Similarly, on the right side of the figure, DAMAS results for the low noise chevron nozzle set for both unshielded (Fig. 14b) and shielded cases (Figs. 14c and 14e) are presented. Thus, the nozzle effect is observed in the rows while the shielding effect is observed in either column. The underside of the HWB is shown in each map as well as a view of the nozzles, looking through the fuselage surface if necessary. The total sound pressure levels reported at the top of each figure represent integrated SPL over the entire source region. Note that the total noise reduction of the shielded low noise chevron nozzles (Fig.14a-14e = 7.3 dB) is greater than the sum of the nozzle benefit (Fig.14a-14b = 1.4 dB) and the shielding benefit (Fig.14a-14d = 4.7 dB) of the axisymmetric nozzle. This is because the chevron nozzles not only reduce noise, they also shift the peak noise source distribution toward the upstream direction, making shielding more effective. This peak noise source re-distribution is evident when comparing the maps across the top row of Fig. 14 and was also observed in previous studies[6-8].

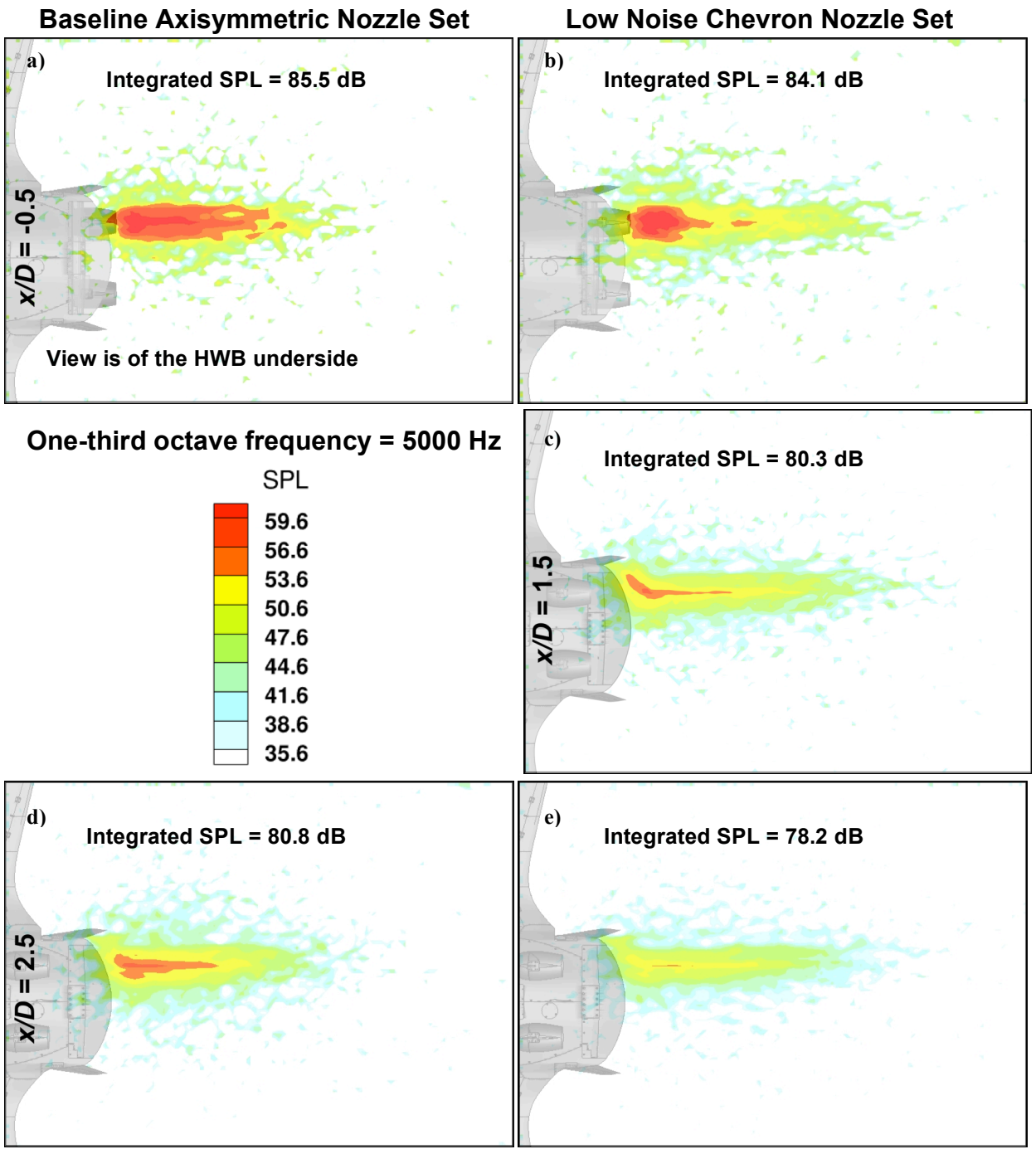

Figure 14. Phased array results with DAMAS processing showing noise source maps at f = 5000 Hz one-third-octave band for port CJES operating, cutback conditions, M_{wt} = 0.17. Results for the a) unshielded axisymmetric nozzle set, b) unshielded chevron nozzle set, c) shielded (x/D = 1.5) chevron nozzle set, d) shielded (x/D = 2.5) axisymmetric nozzle set, and e) shielded (x/D = 2.5) chevron nozzle set are shown.

Figure 15 shows the source maps for the same conditions as Fig. 14 except at the 10,000 Hz one-third-octave band. In this higher frequency case, peak noise is more concentrated near the nozzle exit; thus, the shielding benefit is more pronounced. On the other hand, the nozzle benefit from the chevrons is minimal at higher frequencies, until the source is shielded. Figure 15 shows a 5.2 dB benefit to shielding for the axisymmetric nozzle compared to an 8.3 dB benefit for the chevron nozzle, even though there is no difference in integrated levels over the source region for the unshielded nozzle comparison.

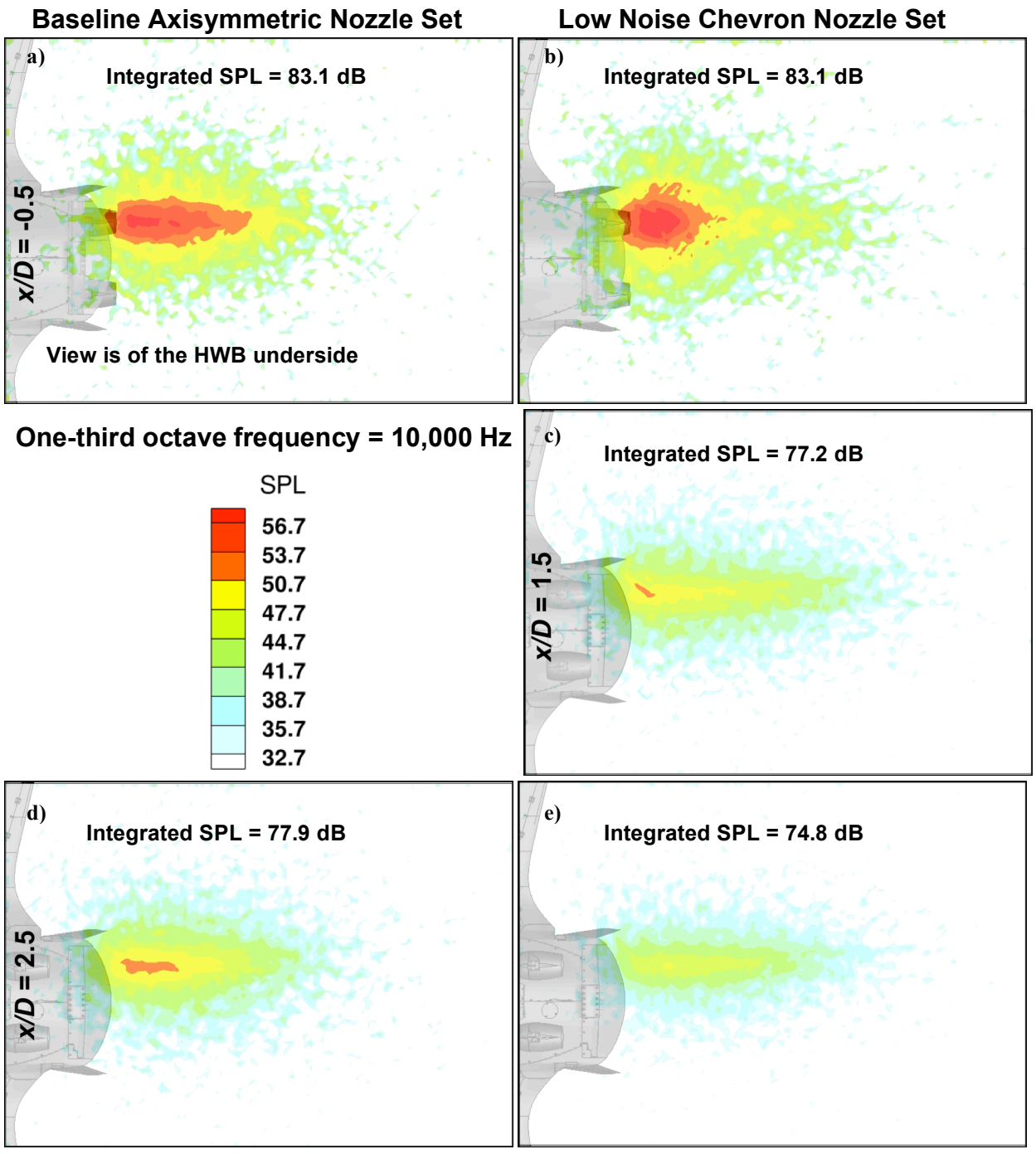

Figure 15. Phased array results with DAMAS processing showing noise source maps at f = 10,000 Hz one-third-octave band for port CJES operating, cutback conditions, M_{wt} = 0.17. Results for the a) unshielded axisymmetric nozzle set, b) unshielded chevron nozzle set, c) shielded (x/D = 1.5) chevron nozzle set, d) shielded (x/D = 2.5) axisymmetric nozzle set, and e) shielded (x/D = 2.5) chevron nozzle set are shown.

Likewise in Fig. 16, the phased array results for the 20,000 Hz one-third-octave band are displayed. Although there is a slight increase in noise for the unshielded chevron nozzle compared to the axisymmetric nozzle of 0.5 dB, the shielding benefit for the chevron nozzle outweighs this increase. The axisymmetric nozzle shows a 5.9 dB benefit due to shielding while the chevron nozzle shows a 9.2 dB benefit.

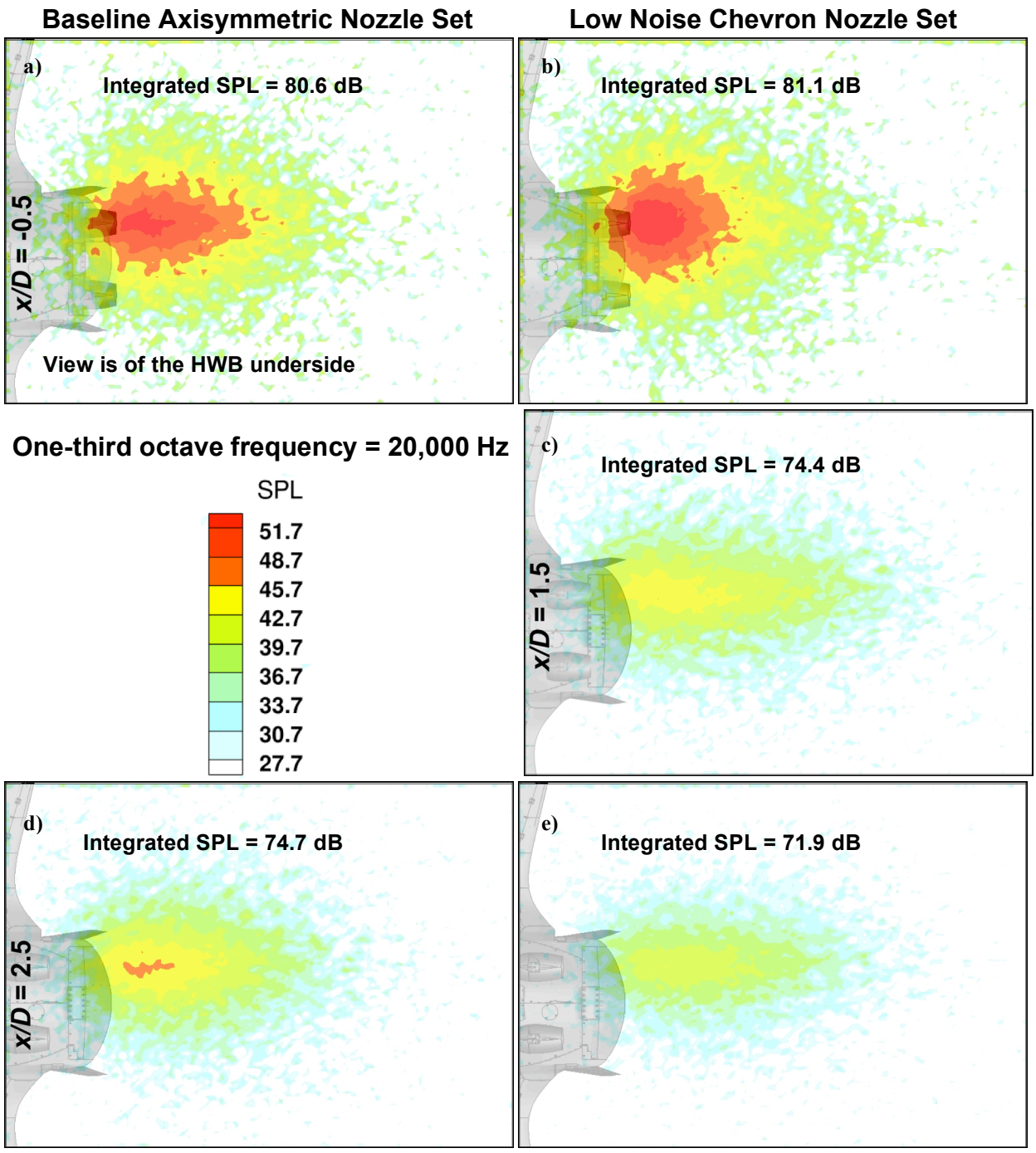

Figure 16. Phased array results with DAMAS processing showing noise source maps at f = 20,000 Hz one-third-octave band for port CJES operating, cutback conditions, M_{wt} = 0.17. Results for the a) unshielded axisymmetric nozzle set, b) unshielded chevron nozzle set, c) shielded (x/D = 1.5) chevron nozzle set, d) shielded (x/D = 2.5) axisymmetric nozzle set, and e) shielded (x/D = 2.5) chevron nozzle set are shown.

IV. Concluding Remarks

This paper describes the jet noise portion of the recent Hybrid Wing Body (HWB) acoustic test that took place within the 14-by 22-Foot Subsonic Tunnel at NASA Langley Research Center. Two Compact Jet Engine Simulator (CJES) units are mounted underneath the inverted 5.8% scale model of the N2A HWB aircraft designed by Boeing Research and Technology. The CJES units are capable of moving to discrete axial stations under the HWB to investigate varying levels of acoustic shielding. A phased microphone array system is mounted on a traverse system above the test section of the tunnel, and an additional system of microphones are mounted on two towers and the overhead truss system to move with the phased array and more effectively capture the directivity pattern of the generated noise. Both a baseline axisymmetric nozzle set and a low noise asymmetric chevron nozzle set are evaluated with and without the benefit of shielding from the HWB fuselage.

Measurements of noise from the tower/truss system are plotted in a flattened hemisphere format, and measured contours at each of the three HWB cycle points are presented for further use in community noise assessments. Comparisons of the two nozzle sets in an unshielded (x/D = -0.5) configuration show expected jet noise source reduction at lower frequencies on the order of 1 to 2 dB and a penalty of up to 2 dB at higher frequencies. However, the intent of the chevron nozzle design is to maximize noise benefit with the presence of shielding. These results confirm trends observed in Thomas *et al.*[8] for the same nozzle designs.

Comparisons of noise contours for the axisymmetric nozzle set in the shielded (x/D = 2.5) and unshielded configurations show increased shielding benefits for increasing one-third-octave frequency with up to 6.5 dB benefit measured at 20,000 Hz. Noise increases are observed at large azimuthal angles when transitioning to the unshielded half-plane of the nozzle system. The asymmetry of the observed noise increase suggests a reflection path from the port CJES off the vertical tail to the starboard microphones. With the capability to measure the installed vehicle system over a wide range of polar and azimuthal angles, this test can reveal such reflection paths, not previously observed in earlier component level studies. Similar behavior is observed for the chevron nozzle set, but shielding benefits are more pronounced, reaching up to 10 dB at 20,000 Hz. The noise reduction of the shielded chevron nozzle is greater than the additive benefits of shielding and jet source noise reduction because the chevron nozzle also influences the peak noise source location within the jet plume, moving that location closer to the nozzle exit and making it more amenable to shielding.

Phased array measurements are deconvolved with the DAMAS array processing algorithm to permit noise maps of the jet source field. These contour plots effectively show the migration of the peak noise source region upstream toward the nozzle exit for the chevron case. Furthermore, integrated SPL of the noise source region again demonstrate the benefit of the chevron nozzle set to both reduce the source noise at lower frequencies and increase the shielding effectiveness for increased jet noise reduction.

Acknowledgments

The authors sincerely thank the entire 14x22 Tunnel team for their efforts during these experiments. Additionally, the authors thank test engineer Les Yeh and test coordinators Dan Hoad and Stephanie Heath for successful test operations. Furthermore, John Swartzbaugh is recognized for his efforts in CJES operations, Larry Becker and Dan Stead for data acquisition, and Tony Humphreys, Jerry Plassman, and Taylor Spalt for data processing contributions. Florence Hutcheson is also acknowledged for her helpful discussions regarding data presentation. Funding from the Environmentally Responsible Aviation Project within NASA's Integrated Systems Research Program is gratefully acknowledged.

References

[1]Collier, F.S., "Environmentally Responsible Aviation (ERA) Project," presentation at the NASA Fundamental Aeronautics Program, Third Annual Meeting, Atlanta, Georgia, September 29-October 1, 2009.

[2]Lopes, L. V. and Burley, C. L., "Design of the Next Generation Aircraft Noise Prediction Program: ANOPP2," AIAA Paper No. 2011-2854 presented at the 17th AIAA/CEAS Aeroacoustics Conference, June 2011.

[3]Doty, M. J., and Haskin, H. H., "Investigation of Flow Conditioners for Compact Jet Engine Simulator Rig Noise Reduction," AIAA Paper No. 2011-2791 presented at the 17th AIAA/CEAS Aeroacoustics Conference, June 2011.

[4]Doty, M. J., and Haskin, H. H., "Acoustic Characterization of Compact Jet Engine Simulator Units," AIAA Paper No. 2013-2035, 19th AIAA/CEAS Aeroacoustics Conference, May 2013.

[5]Hill, G.A., Brown, S.A., Geiselhart, K.A., and Burg, C.M., "Integration of Propulsion Airframe Aeroacoustic Technologies and Design Concepts for a Quiet Blended Wing Body Transport," AIAA Paper No. 2004-6306 presented at the 10th AIAA/CEAS Aeroacoustics Conference, May 2004.

[6]Czech, M.J., Thomas, R.H., and Elkoby, R., "Propulsion Airframe Aeroacoustic Integration Effects of a Hybrid Wing Body Aircraft Configuration," *International Journal of Aeroacoustics*, Vol. 11, No. 3+4, 2012, pp. 335-368.

[7]Thomas, R. H., Burley, C. L., and Olson, E.D., "Hybrid Wing Body System Noise Assessment with Propulsion Airframe Aeroacoustic Experiments," *International Journal of Aeroacoustics*, Vol. 11, No. 3+4, 2012, pp. 369-410.

[8]Thomas, R. H., Czech, M. J., and Doty, M. J., "High Bypass Ratio Jet Noise Reduction and Installation Effects Including Shielding Effectiveness," AIAA Paper No. 2013-0541 presented at the 51st AIAA Aerospace Sciences Meeting, January 2013.

[9]Heath, S. L., Brooks, T. F., Hutcheson, F. V., Doty, M. J., Haskin, H. H., Spalt, T. B., Bahr, C. J., Burley, C. L., Bartram, S. M., Humphreys, W. M., Jr., Lunsford, C. B., Popernack, T. G., Colbert, S. E., Hoad, D. R., Becker, L. E., Stead, D. J., Kuchta, D., and Yeh, L., "Hybrid Wing Body Aircraft Acoustic Test Preparations and Facility Upgrades," AIAA Paper No. 2013-2623 presented at the 28th AIAA Aerodynamic Measurement Technology, Ground Testing, and Flight Testing Conference, June 2013.

[10]Heath, S. L., Brooks, T. F., Hutcheson, F. V., Doty, M. J., Bahr, C. J., Hoad, D. R., Becker, L. E., Humphreys, W. M., Jr., Burley, C. L., Stead, D. J., Pope, D. S., Spalt, T. B., Kuchta, D., and Plassman, G. E., "NASA Hybrid Wing Body Aircraft Aeroacoustic Data Report," NASA/TM, 2014 (to be published).

[11]Humphreys, W. M., Jr., Brooks, T. F., Bahr, C. J., Spalt, T. B., Bartram, S. M., Culliton, W. G., and Becker, L. E., "Development of a Microphone Phased Array Capability for the Langley 14- by 22 Foot-Subsonic Tunnel," AIAA paper accepted for presentation at the 20th AIAA/CEAS Aeroacoustics Conference/AIAA Aviation and Aeronautics Forum and Exposition in Atlanta, GA, June 16-20, 2014.

[12]Spalt, T. B., Brooks, T. F., Bahr, C. J., Plassman, G. E., Becker, L. E., and Stead, D. J., "Calibrations of the NASA Langley 14- by 22-Foot Subsonic Tunnel in Acoustic Configuration," AIAA paper accepted for presentation at the 20th AIAA/CEAS Aeroacoustics Conference/AIAA Aviation and Aeronautics Forum and Exposition in Atlanta, GA, June 16-20, 2014.

[13]Bahr, C. J., Brooks, T. F., Humphreys, W. M., Jr., Spalt, T. B., and Stead, D. J., "Acoustic Data Processing and Transient Signal Analysis for the Hybrid Wing Body 14- by 22-Foot Subsonic Wind Tunnel Test," AIAA paper accepted for presentation at the 20th AIAA/CEAS Aeroacoustics Conference/AIAA Aviation and Aeronautics Forum and Exposition in Atlanta, GA, June 16-20, 2014.

[14]Sutliff, D. L. and Walker, B. E., "Shielding Characteristics using an Ultrasonic Configurable Artificial Noise Source to Generate Modes – Experimental Measurements and Analytical Predictions," AIAA paper accepted for presentation at the 20th AIAA/CEAS Aeroacoustics Conference/AIAA Aviation and Aeronautics Forum and Exposition in Atlanta, GA, June 16-20, 2014.

[15]Hutcheson, F. V., Brooks, T. F., Burley, C. L., Bahr, C. J., Stead, D. J., and Pope, D. S., "Shielding of Turbomachinery Noise from a Hybrid Wing Body Aircraft Configuration," AIAA paper accepted for presentation at the 20th AIAA/CEAS Aeroacoustics Conference/AIAA Aviation and Aeronautics Forum and Exposition in Atlanta, GA, June 16-20, 2014.

[16]Burley, C. L., Brooks, T. F., Hutcheson, F. V., Doty, M. J., Lopes, L. V., Nickol, C. L., Vicroy, D. D., and Pope, D. S., "Noise Scaling and Community Noise Metrics for the Hybrid Wing Body Aircraft," AIAA paper accepted for presentation at the 20th AIAA/CEAS Aeroacoustics Conference/AIAA Aviation and Aeronautics Forum and Exposition in Atlanta, GA, June 16-20, 2014.

[17]NASA Langley Ground Facilities and Testing Directorate (GFTD) Facility Fact Sheets, http://gftd.larc.nasa.gov/references/14x22_factsheet.pdf [retrieved October 29, 2013].

[18]Zelina, J., Ehret, J., Hancock, R. D., Shouse, D. T., Roquemore, W. M., and Sturgess, G. J., "Ultra-Compact Combustion Technology Using High Swirl For Enhanced Burning Rate," AIAA Paper No. 2002-3725 presented at the 38th AIAA/ASME/SAE/ASEE Joint Propulsion Conference and Exhibit, July 2002.

[19]Amiet, R. K., "Refraction of Sound by a Shear Layer," *Journal of Sound and Vibration,* Vol. 58, No. 3, 1978, pp. 467-482.

[20]"Calculation of the Absorption of Sound by the Atmosphere," ANSI S1.26-1995 (R2009) American Nat. Stand. Inst., Inc., 1995.

[21]Brooks, T. F., and Humphreys, W. M., Jr., "A Deconvolution Approach for the Mapping of Acoustic Sources (DAMAS) Determined from Phased Microphone Arrays", *Journal of Sound and Vibration*, Vol. 294, 2006, pp. 856-879.

[22]Brooks, T. F., Humphreys, W. M., Jr., and Plassman, G. E., "DAMAS Processing for a Phased Array Study in the NASA Langley Jet Noise Laboratory," AIAA Paper No. 2010-3780 presented at the 16th AIAA/CEAS Aeroacoustics Conference, June 2010.